Supporting Information

Facile template-guided synthesis of conformal Bi_2O_3-coated $LiMn_2O_4$ hollow microspheres for enhanced stability of lithium-ion battery cathodes

Iyan Subiyanto,[a,b] Winda Devina,[c] Segi Byun,[a,b] and Hyunuk Kim*[b,c,d]*

[a]Energy Storage Research Department, Korea Institute of Energy Research, 152 Gajeong-ro, Yuseong-gu, Daejeon, 34129, Republic of Korea

[b]Energy Engineering, University of Science and Technology, 217 Gajeong-ro, Yuseong-gu, Daejeon, 34113, Republic of Korea

[c]CCS Research Department, Korea Institute of Energy Research, 152 Gajeong-ro, Yuseong-gu, Daejeon, 34129, Republic of Korea

[d]Department of Advanced Materials Chemistry, Korea University, 2511 Sejong-ro, Sejong, 30019, Republic of Korea

[*]To whom correspondence should be addressed:

e-mail: segibyun@kier.re.kr, hukim@korea.ac.kr

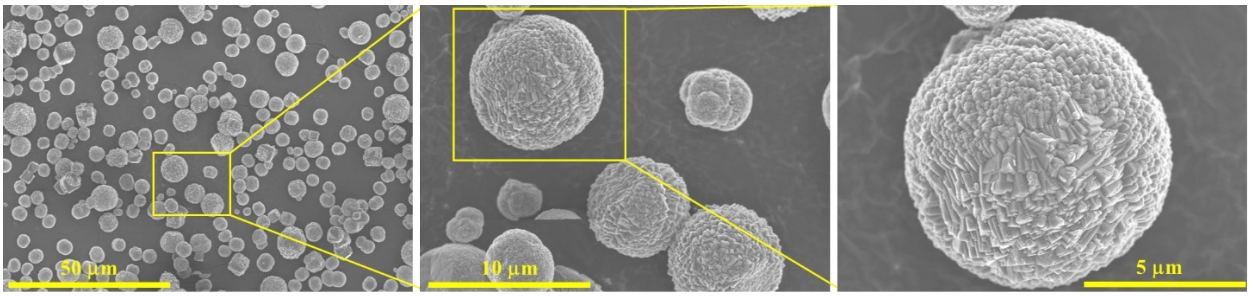

Fig. S1 SEM images showing the morphology of $MnCO_3$ microspheres as an intermediate product.

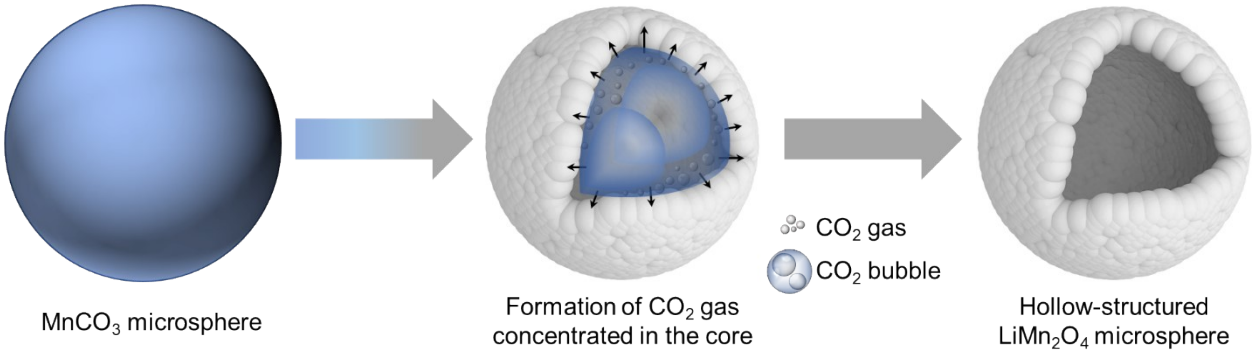

Fig. S2 Schematic illustration of the growth mechanism for $LiMn_2O_4$ hollow microspheres.

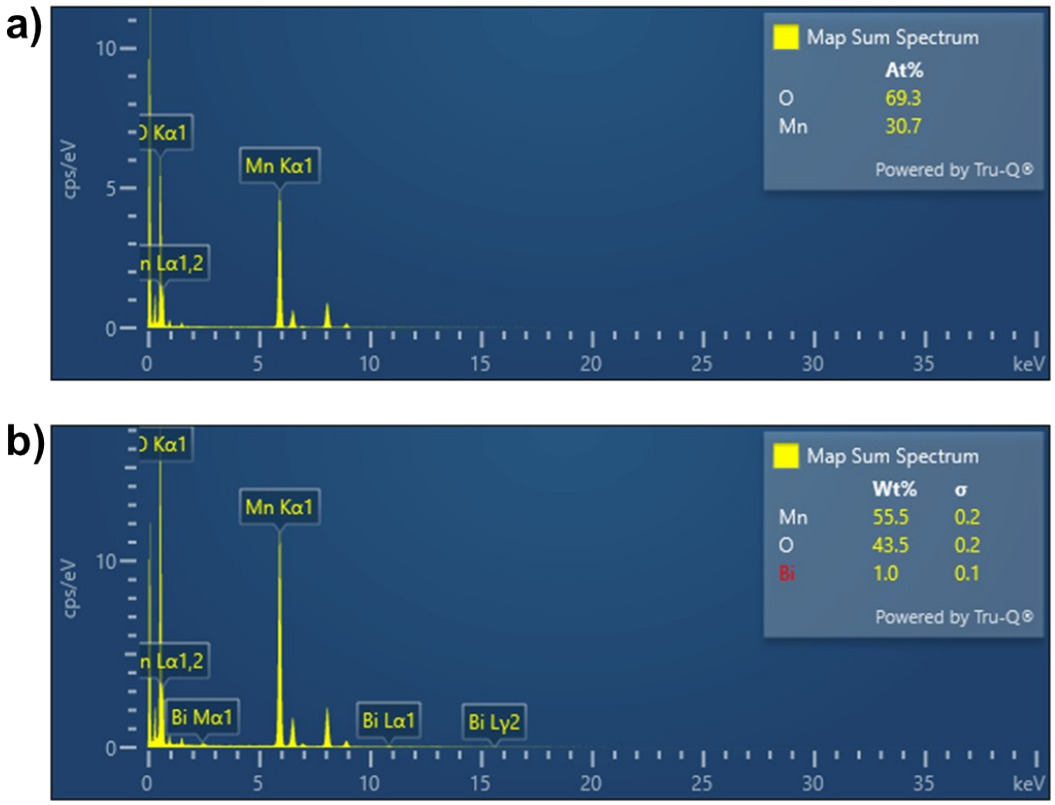

Fig. S3 EDS spectra of (a) LMOhms, and (b) BiLMOhms detect the Bi loading amount during TEM measurement.

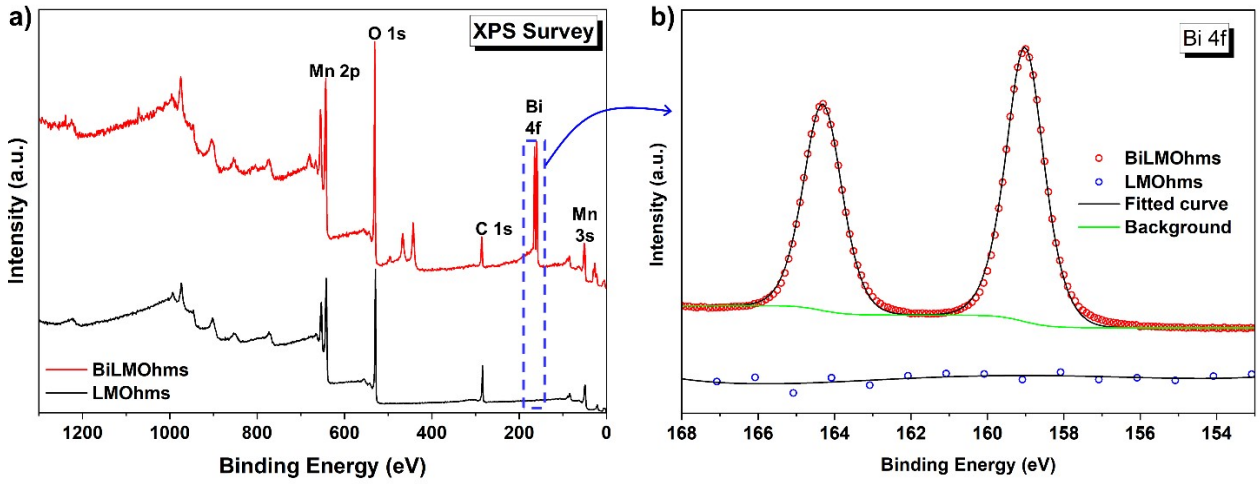

Fig. S4 XPS spectra of BiLMOhms compared to pristine LMOhms. (a) XPS survey spectra, (b) the enlarge spectra of the Bi 4f peak, as indicated by the blue rectangular area.

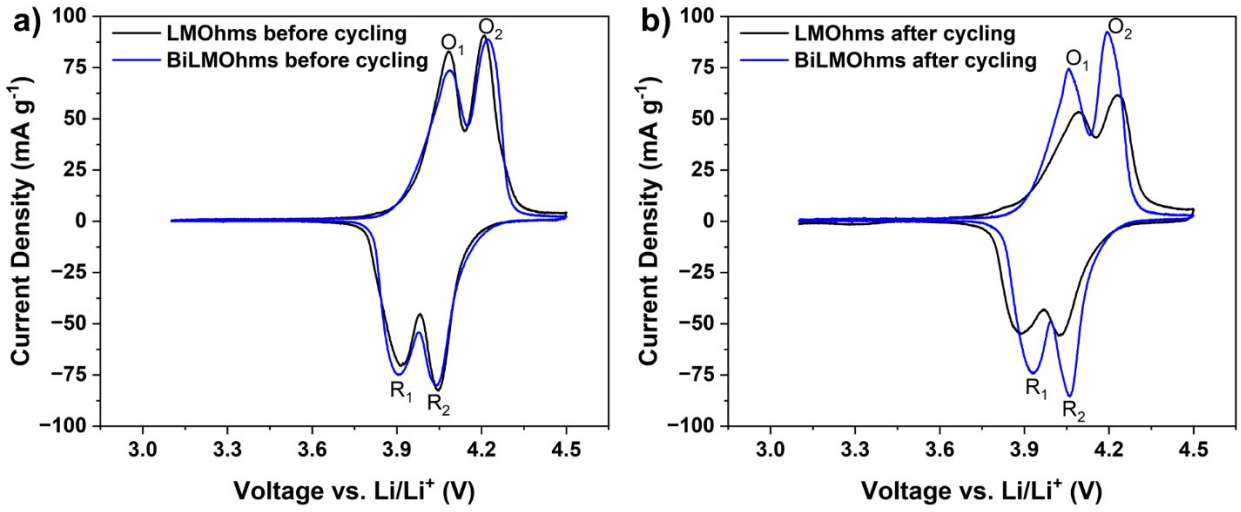

Fig. S5 Cyclic voltammetry of BiLMOhms and pristine LMOhms in half-cell configuration: (a) before cycling, and (b) after 50 cycles.

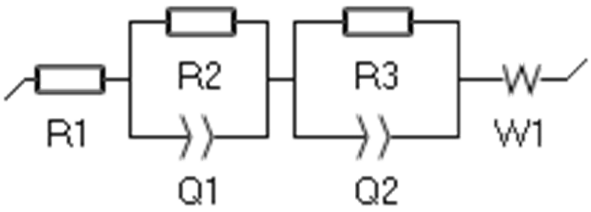

Fig. S6 Equivalent circuit model used for EIS data fitting. R_1 represents the solution resistance (R_s), corresponding to the bulk resistance of the electrolyte. R_2 denotes the surface film resistance (R_{sf}), corresponding to thin interfacial layers such as the coating layer or the cathode–electrolyte interface (CEI). R_3 is the charge transfer resistance (R_{ct}), associated with the Li^+ insertion/extraction process. W_1 represents the Warburg impedance, reflecting Li^+ diffusion within the bulk of the cathode material.

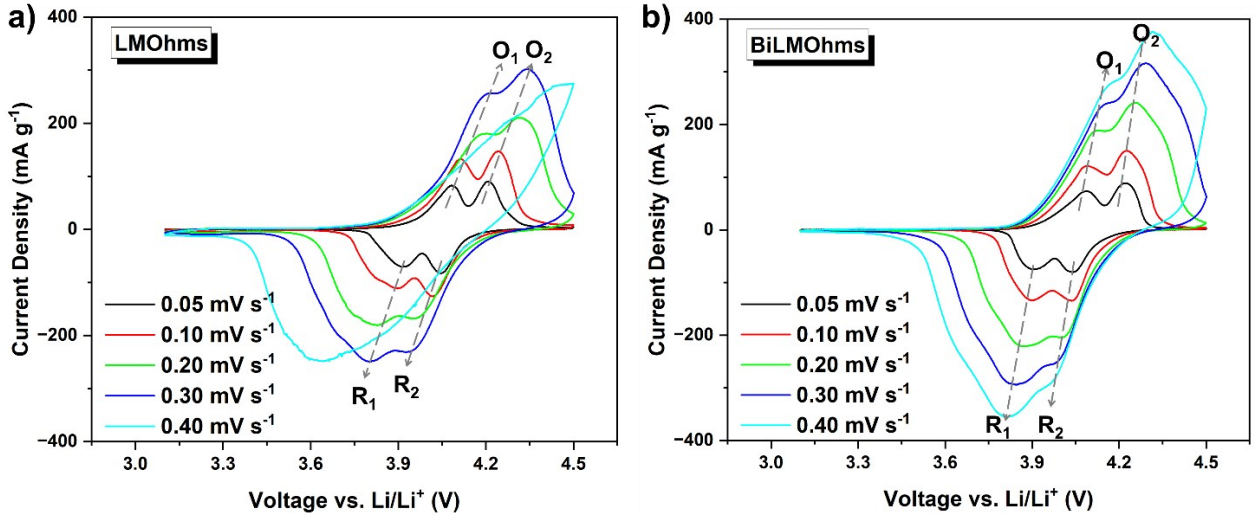

Fig. S7 Cyclic voltammetry at different scan rate of (a) LMOhms and (b) BiLMOhms.

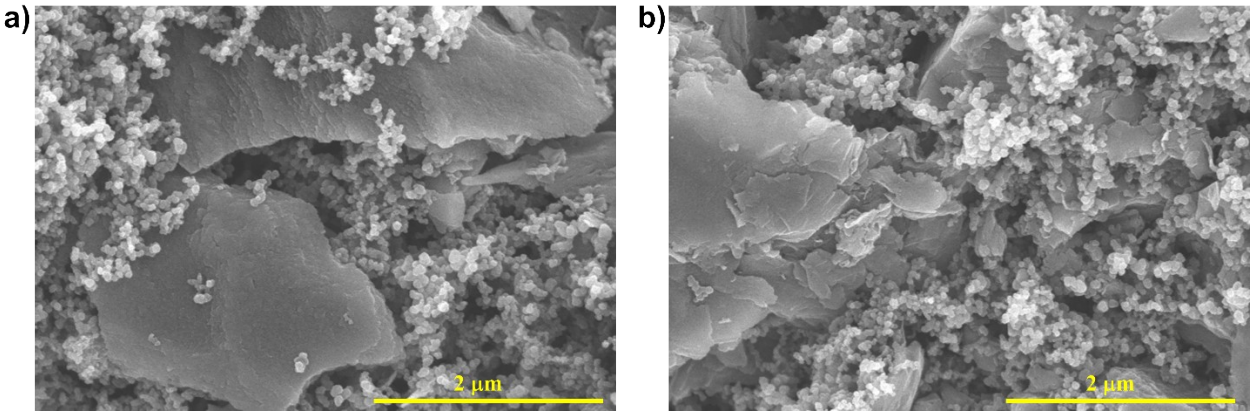

Fig. S8 SEM images of graphite anodes before cycling: (a) from the LMOhms||Graphite cell and (b) from the BiLMOhms||Graphite cell.

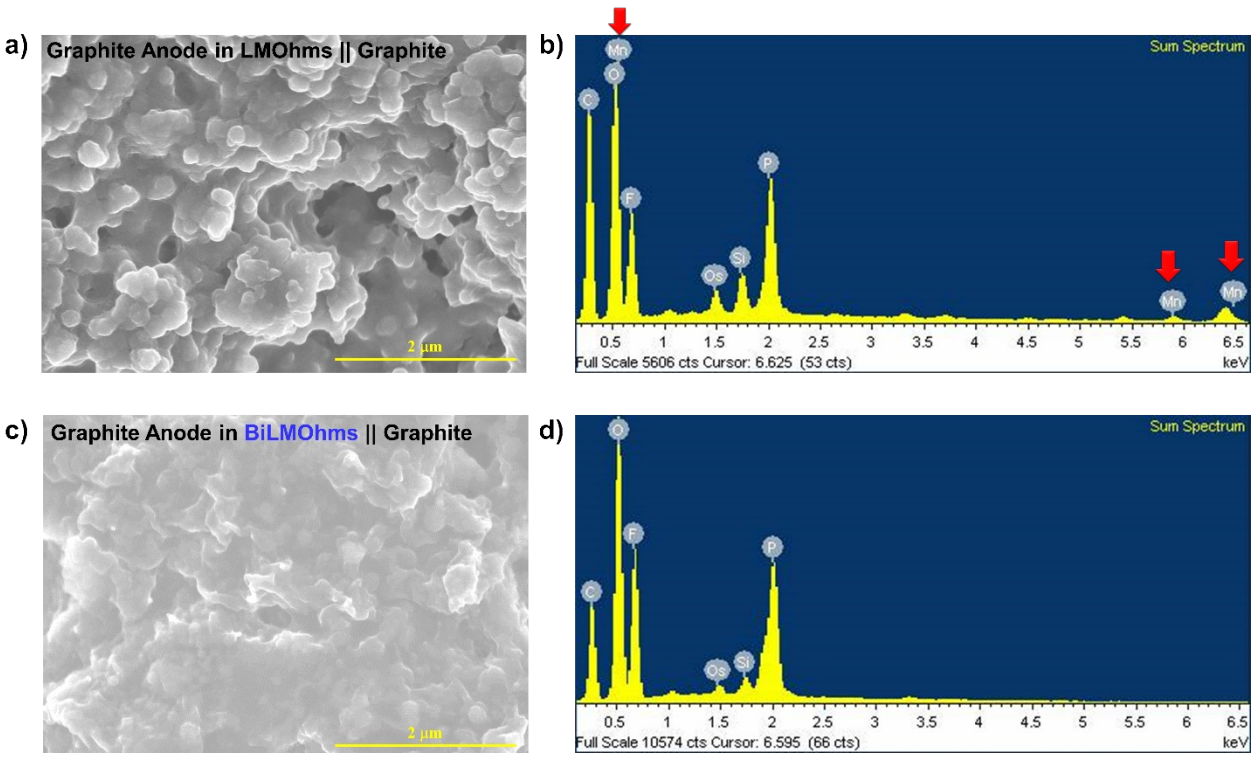

Fig. S9 Post-mortem analysis of graphite anodes after long-term cycling. (a) SEM image of the graphite anode from the LMOhms‖Graphite cell and its (b) EDS spectrum. (c) SEM image of the graphite anode from the BiLMOhms‖Graphite cell and its (d) EDS spectrum.

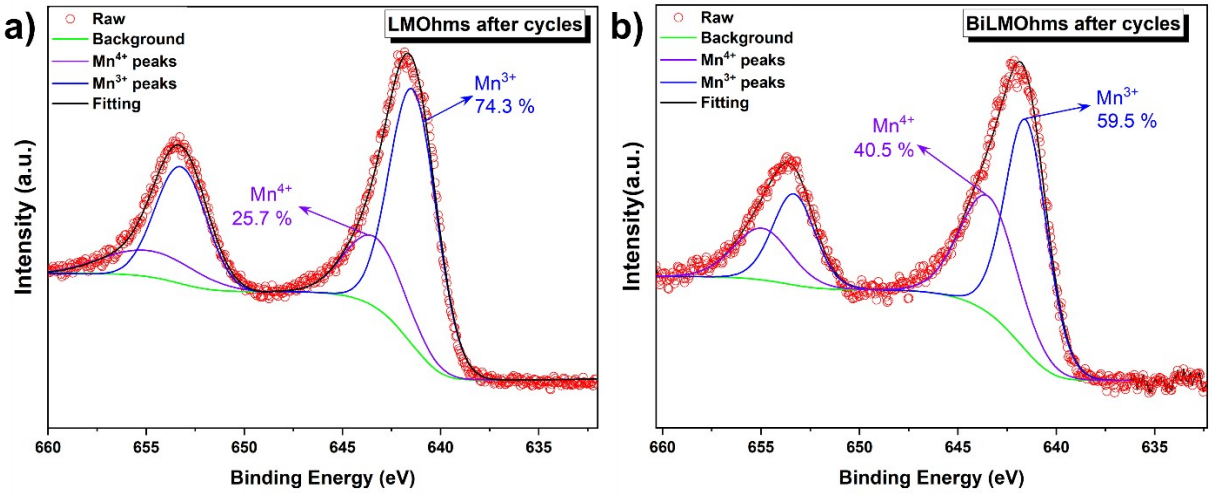

Fig. S10 Post-mortem analysis of XPS spectra after cycles: (a) LMOhms, and (b) BiLMOhms.

Table S1. Elemental composition of LMOhms and BiLMOhms determined by inductively coupled plasma (ICP) analysis.

Element	$LiMn_2O_4$		Bi_2O_3-$LiMn_2O_4$	
Bi	< 0.01 wt.%		1.18 wt.%	0.005 at.%
Li	3.98 wt.%	0.57 at.%	3.98 wt.%	0.57 at.%
Mn	57.9 wt.%	1.05 at.%	61.4 wt.%	1.12 at.%

Table S2. Electrochemical half-cell performance of $LiMn_2O_4$ cathodes with various surface coating materials reported in the literature for comparison.

No	Coating Material	Initial specific capacity (mAh g^{-1})	C-rate (C)	No. of cycle(N)	Capacity retention (pristine/coated)	Retention enhancement	Ref.
1	$LiTaO_3$	103.0	2.03	500	65.7% / 95.0 %	29.3%	1
2	Li_3PO_4	125.0	1	300	80.8% / 90.8%	10.0%	2
3	$MnBO_3$	112.7	1	1000	56.8% / 85.2%	28.4%	3
4	Al_2O_3/ZrO_2 composite	113.6	1	100	97.4% / 98.7%	1.3%	4
5	Al_2O_3	120.4	1	100	72.9% / 93.5%	20.6%	5
6	ZnO	97.5	0.5	500	57.5% / 84.1%	26.6%	6
7	TiO_2	127.3	0.5	250	80.3% / 90.1%	9.8%	7
8	$LaBO_3$	119.4	1	200	76.8% / 89.5%	12.7%	8
9	Sm_2O_3	101.6	1	200	76.3% / 94.7%	18.4%	9
10	Li_2MnO_3	113.3	1	500	72.1% / 94.2%	22.1%	10
11	F-SnO_2	114.9	1	100	84.1% / 97.1%	13.0%	11
12	Carbon	103.6	0.75	1000	76.0% / 82.0%	6.0%	12
13	PEDOT	115.0	1	100	79.0% / 83.0%	4.0%	13
14	PVDF	112.4	0.75	500	67.7% / 80.0%	12.3%	14
15	**Bi_2O_3**	**97.4**	**1**	**1000**	**45.8% / 80.1%**	**34.3%**	**This work**

Table S3. Electrochemical performance of $LiMn_2O_4$||Graphite full cells reported in the literature for comparison.

No	Sample label	C-rate (C)	No. of cycle(N)	Capacity retention (pristine/threated)	Retention enhancement	Ref.
1	LMO@C	1	900	46.1% / 67.2%	21.1%	15
2	LR-LMO	0.1	50	69.0% / 86.0%	17.0%	16
3	CoLi-LMO	2	300	62.0% / 94.0%	32.0%	17
4	CXL-LMO	1	500	73.0% / 84.0%	11.0%	18
5	**BiLMOhms**	**1**	**100**	**39.6% / 87.4%**	**47.8%**	**This work**

Table S4. Elemental composition of LMOhms and BiLMOhms determined by XPS.

$LiMn_2O_4$ (LMOhms)				Bi_2O_3-$LiMn_2O_4$ (BiLMOhms)			
Name	Peak BE	Area (P) CPS.eV	at. %	Name	Peak BE	Area (P) CPS.eV	at. %
Li1s	62.93	7218.56	7.66	Li1s	54.29	1499.63	7.63
Mn2p	642.61	2444379.73	19.08	Mn2p	642.57	527113.24	18.76
O1s	529.92	1435481.28	43.74	O1s	529.98	298064.48	50.25
C1s	284.80	400016.72	29.51	C1s	284.80	54023.33	3.07
				Bi4f	159.07	152797.39	20.29

References

1. H. Li, N. Chen, S. Zhang, Y. Han, X. Gao, H. Chen, Y. Bai and W. Gao, Fast-Ion Conductor Coating Strategy Modified $LiMn_2O_4$ for Rocking-Chair Lithium-Ion Capacitors, *ACS Applied Materials & Interfaces*, 2025, **17**, 21269-21280.
2. J. Wang, Y. Xu, Y. Niu, Y. Liu and X. Yao, Lithium-Ion Conductivity Epitaxial Layer Contributing to the Structure and Cycling Stability of $LiMn_2O_4$ Cathodes, *ACS Sustainable Chemistry & Engineering*, 2023, **11**, 5408-5419.
3. H. Li, L. Xue, M. Ni, S. V. Savilov, S. M. Aldoshin and H. Xia, Boosting the cycling performance of spinel $LiMn_2O_4$ by in situ $MnBO_3$ coating, *Electrochemistry Communications*, 2022, **137**, 107266.
4. S. Wang, C. Luo, Y. Feng, G. Fan, L. Feng, M. Ren and B. Liu, Electrochemical properties and microstructures of $LiMn_2O_4$ cathodes coated with aluminum zirconium coupling agents, *Ceramics International*, 2020, **46**, 13003-13013.
5. H. Liu, F. Yang, J. Guo, M. Xiang, H. Bai, R. Wang and C. Su, Facile combustion synthesis of amorphous Al_2O_3-coated $LiMn_2O_4$ cathode materials for high-performance Li-ion batteries, *New Journal of Chemistry*, 2021, **45**, 10534-10540.
6. Q.-L. Li, W.-Q. Xu, H.-L. Bai, J.-M. Guo and C.-W. Su, ZnO-coated $LiMn_2O_4$ cathode material for lithium-ion batteries synthesized by a combustion method, *Ionics*, 2016, **22**, 1343-1351.
7. C. Zhang, X. Liu, Q. Su, J. Wu, T. Huang and A. Yu, Enhancing Electrochemical Performance of $LiMn_2O_4$ Cathode Material at Elevated Temperature by Uniform Nanosized TiO_2 Coating, *ACS Sustainable Chemistry & Engineering*, 2017, **5**, 640-647.
8. Y. Chen, Z. Qian, Q. Zhu, L. Xia, W. Bai, M. Xiang, Y. Guo, S. Chou, P. Ning and J. Guo, A modification engineering to form two kinds of truncated octahedrons by in situ $LaBO_3$ coating for high-performance $LiMn_2O_4$ cathode material, *Materials Today Chemistry*, 2024, **38**, 102047.
9. B. Zhang, Y. Zhang, B. Zhu, J. Duan, X. Li, X. Zeng, Z. Lian, R. Gong, K. Zhou, Z. Wang, Y. Gao, P. Dong and Y. Zhang, Beneficial impact of incorporating spinel lithium manganate and samarium oxide into high performance positive materials through ultrasonic cavitation strategy, *Colloids and Surfaces A: Physicochemical and Engineering Aspects*, 2022, **646**, 128985.
10. Z. Peng, G. Wang, Y. Cao, Z. Zhang, K. Du and G. Hu, Enhanced high power and long life performance of spinel $LiMn_2O_4$ with Li_2MnO_3 coating for lithium-ion batteries, *Journal of Solid State Electrochemistry*, 2016, **20**, 2865-2871.
11. D.-Y. Shin, B.-R. Koo and H.-J. Ahn, Lithium storage kinetics of highly conductive F-doped SnO_2 interfacial layer on lithium manganese oxide surface, *Applied Surface Science*, 2020, **499**, 144057.
12. V. Selvamani, N. Phattharasupakun, J. Wutthiprom and M. Sawangphruk, High-performance spinel $LiMn_2O_4$@carbon core–shell cathode materials for Li-ion batteries, *Sustainable Energy & Fuels*, 2019, **3**, 1988-1994.
13. L. Su, P. M. Smith, P. Anand and B. Reeja-Jayan, Surface Engineering of a $LiMn_2O_4$ Electrode Using Nanoscale Polymer Thin Films via Chemical Vapor Deposition Polymerization, *ACS Applied Materials & Interfaces*, 2018, **10**, 27063-27073.

14. C. L. Mu, M. Huang, H. L. Zhu, Y. X. Qi, Y. X. Wang, T. Li and Y. J. Bai, Promoting the electrochemical performance of commercial $LiMn_2O_4$ by hydrothermal modification with poly (vinylidene fluoride), *Materials Today Sustainability*, 2022, **18**, 100128.
15. C. Tomon, S. Sarawutanukul, N. Phattharasupakun, S. Duangdangchote, P. Chomkhuntod, N. Joraleechanchai, P. Bunyanidhi and M. Sawangphruk, Core-shell structure of $LiMn_2O_4$ cathode material reduces phase transition and Mn dissolution in Li-ion batteries, *Communications Chemistry*, 2022, **5**, 54.
16. T. Liu, A. Dai, J. Lu, Y. Yuan, Y. Xiao, L. Yu, M. Li, J. Gim, L. Ma, J. Liu, C. Zhan, L. Li, J. Zheng, Y. Ren, T. Wu, R. Shahbazian-Yassar, J. Wen, F. Pan and K. Amine, Correlation between manganese dissolution and dynamic phase stability in spinel-based lithium-ion battery, *Nature Communications*, 2019, **10**, 4721.
17. C. Wang, S. Lu, S. Kan, J. Pang, W. Jin and X. Zhang, Enhanced capacity retention of Co and Li doubly doped $LiMn_2O_4$, *Journal of Power Sources*, 2009, **189**, 607-610.
18. U. Pal, B. Roy, M. Hasanpoor, H. Ilbeygi, T. Mendes, R. Kerr, L. Vazhapully, C. Song, D. Wang, M. Boot-Handford, M. G. Sceats, M. Forsyth, D. Al-Masri and P. C. Howlett, Developing a High-Performing Spinel $LiMn_2O_4$ Cathode Material with Unique Morphology, Fast Cycling and Scaled Manufacture, *Batteries & Supercaps*, 2024, **7**, e202400072.